

Research Article

Optical, X-Ray Diffraction, and Magnetic Properties of the Cobalt-Substituted Nickel Chromium Ferrites ($\text{CrCo}_x\text{Ni}_{1-x}\text{FeO}_4$, $x = 0, 0.2, 0.4, 0.6, 0.8, 1.0$) Synthesized Using Sol-Gel Autocombustion Method

Sonal Singhal,¹ Santosh Bhukal,¹ Jagdish Singh,² Kailash Chandra,² and S. Bansal³

¹Department of Chemistry, Panjab University, Chandigarh 160 014, India

²Institute Instrumentation Centre, IIT Roorkee, Roorkee 247 667, India

³School of Physics and Materials Science, Thapar University, Patiala 147004, India

Correspondence should be addressed to Sonal Singhal, sonal1174@gmail.com

Received 9 March 2011; Accepted 28 March 2011

Academic Editor: Mallikarjuna Nadagouda

Copyright © 2011 Sonal Singhal et al. This is an open access article distributed under the Creative Commons Attribution License, which permits unrestricted use, distribution, and reproduction in any medium, provided the original work is properly cited.

Cobalt-substituted nickel chromium ferrites ($\text{CrCo}_x\text{Ni}_{1-x}\text{FeO}_4$, $x = 0, 0.2, 0.4, 0.6, 0.8, 1.0$) have been synthesized using sol-gel autocombustion method and annealed at 400 °C, 600 °C, 800 °C, and 1000 °C. All the ferrite samples have been characterized using UV-VIS spectrophotometry, FT-IR spectroscopy, Transmission Electron Microscopy, powder X-Ray Diffraction, and magnetic measurements. Typical FT-IR spectra of the samples annealed at 400 °C, 600 °C, 800 °C, and 1000 °C exhibit two frequency bands in the range of $\sim 480\text{ cm}^{-1}$ and $\sim 590\text{ cm}^{-1}$ corresponding to the formation of octahedral and tetrahedral clusters of metal oxide, respectively. TEM images reveal that crystallite size increases from $\sim 10\text{ nm}$ to $\sim 45\text{ nm}$ as the annealing temperature is increased from 400 °C to 1000 °C. The unit cell parameter “a” is found to increase on increasing the cobalt concentration due to larger ionic radius of cobalt. Also, as the cobalt concentration increases, the saturation magnetization increases from 4.32 to 19.85 emu/g. This is due to the fact that cobalt ion replaces the less magnetic nickel ions. However, the coercivity decreases with increase in cobalt concentration due to the decrease in anisotropy field. The band gap has been calculated using UV-VIS spectrophotometry and has been found to decrease with the increase of particle size.

1. Introduction

Magnetic nanoferrite particles have generated diverse technological interests because of their potential applications in magnetic fluids, high frequency magnets, magnetic bulk cores, microwave absorbers, and high-density data storage [1, 2]. Among the various ferrites, nickel ferrites and cobalt ferrites have been extensively used in electronic devices because of their large permeability at high frequency, remarkably high electrical resistivity, mechanical hardness, chemical stability, and cost-effectiveness [3, 4]. Substituted nickel ferrites are widely used as magnetic materials due to their high electrical resistivity, low eddy current, and dielectric losses [5, 6].

The magnetic properties of materials are strongly affected when the particle size approaches a critical diameter, below

which each particle is a single domain. As a result the influence of thermal energy over the magnetic moment ordering leads to super paramagnetic relaxation [7, 8]. Cobalt and nickel, both the ferrites, belong to the category of inverse spinel ferrites. Therefore, by substituting the Co^{2+} , Ni^{2+} , and/or Fe^{3+} ions by suitable cations, their structures undergo a change from inverse spinel to mixed spinel, leading to a corresponding change in the magnetic properties. Thus, by the choice of the cations as well as their distribution in tetrahedral and octahedral sites of the lattice, interesting and useful magnetic properties can be obtained [9].

The effect of substitution of Fe^{3+} by Cr^{3+} in NiFe_2O_4 has been studied by various workers [10–12], and it has been reported that Cr^{3+} always seeks to the octahedral sites. Lee et al. [10] suggested that Ni^{2+} moves to tetrahedral site within the range $0.2 < x < 0.6$ and the magnetic moment and Curie

temperature decrease with the chromium substitution. Fayek and Ata Allah [11] reported that Cr^{3+} occupies the octahedral sites for a maximum of $x = 0.6$ and the excess Cr^{3+} replaces the Fe^{3+} at the tetrahedral site. Gismelseed and Yousif [12] studied the Cr^{3+} substituted $\text{NiCr}_x\text{Fe}_{1-x}\text{O}_4$ ($0 < x < 1.4$) prepared through conventional double sintering ceramic technique and suggested that as the Cr^{3+} substitution increases, the system is slowly converted into a normal spinel structure.

Chae et al. [13] reported the magnetic properties of chromium substituted cobalt ferrites prepared using sol-gel method and suggested that the coercivity decreases fast but saturation magnetization decreases slowly with the chromium content. Gabal and Al Angari [14] reported the effect of chromium ion substitution on the electromagnetic properties of nickel ferrite and observed that coercivity increases, whereas the saturation magnetization decreases linearly with the Cr content. They also reported that the Neel's magnetic moments calculated from expected cation distribution are in confirmation with those obtained from the hysteresis loops for ferrites up to $x = 0.8$.

The present work deals with the synthesis of nanoparticles of cobalt-substituted nickel chromium ferrites ($\text{CrCo}_x\text{Ni}_{1-x}\text{FeO}_4$, where $x = 0, 0.2, 0.4, 0.6, 0.8$ & 1.0) via sol-gel autocombustion method and investigation of their optical, X-ray diffraction, and magnetic properties by means of FT-IR, UV-Vis spectrophotometry, Powder X-ray diffraction, and magnetic measurements.

2. Experimental

2.1. Preparation of $\text{CrCo}_x\text{Ni}_{1-x}\text{FeO}_4$ Nanoparticles. Nanoparticles of $\text{CrCo}_x\text{Ni}_{1-x}\text{FeO}_4$ ($x = 0, 0.2, 0.4, 0.6, 0.8$ & 1.0) have been synthesized by sol-gel autocombustion method [15–17]. AR Grade $\text{Fe}(\text{NO}_3)_3 \cdot 9\text{H}_2\text{O}$, $\text{Co}(\text{NO}_3)_2 \cdot 6\text{H}_2\text{O}$, $\text{Cr}(\text{NO}_3)_3 \cdot 9\text{H}_2\text{O}$, $\text{Ni}(\text{NO}_3)_2 \cdot 6\text{H}_2\text{O}$ and citric acid have been used for the synthesis of these ferrites. The nitrates and citric acid were weighed in desired stoichiometric proportions and dissolved separately in minimum amount of distilled water. The individual solutions were then mixed together and the pH value of the solution was adjusted to about 6 by adding 1 M NH_4OH solution. The solution was then slowly heated and stirred using a hot plate magnetic stirrer till gels were formed, which were ignited and burnt in a self-propagating combustion manner to obtain loose powder. The powders were annealed at 400°C , 600°C , 800°C , and 1000°C in a muffle furnace for 2 hours.

2.2. Physical Measurements. Fourier Transform infrared (FT-IR) spectra have been recorded using Perkin Elmer RX-1 FT-IR spectrophotometer with KBr pellets in the range $4000\text{--}400\text{ cm}^{-1}$. Powder X-ray diffraction studies have been carried out using a Bruker AXS, D8 Advance spectrophotometer with $\text{Cu-K}\alpha$ radiation. Hitachi (H-7500) TEM, operated at 120 kV was used to record the micrographs of the samples. The magnetic properties have been measured at room temperature by a vibrating sample magnetometer (VSM) (155, PAR) up to a magnetic field of $\pm 10\text{ kOe}$. UV-Visible spectrum was recorded using a Hitachi 330 UV-VIS-NIR spectrophotometer.

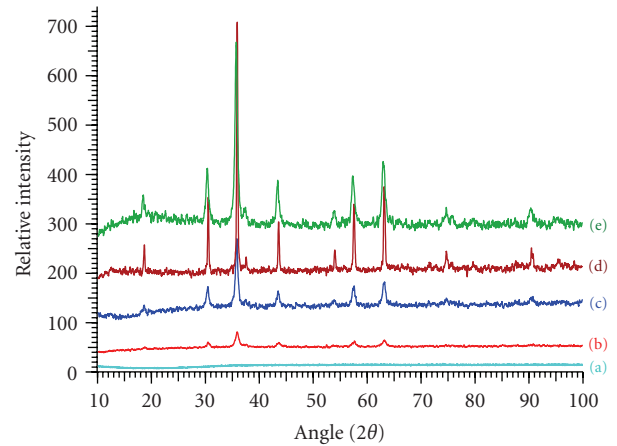


FIGURE 1: X-ray diffraction patterns of $\text{CrCo}_{0.6}\text{Ni}_{0.4}\text{FeO}_4$ (a) as obtained and annealed at (b) 400°C , (c) 600°C , (d) 800°C , and (e) 1000°C .

3. Results and Discussion

3.1. FT-IR Characterization. The FT-IR spectra for all the samples annealed at 400°C , 600°C , 800°C , and 1000°C exhibit two main absorption bands below 1000 cm^{-1} , corresponding to the vibrational modes of the metal oxides of ferrites. The band in the range of $\sim 590\text{ cm}^{-1}$ is attributed to the stretching mode of the tetrahedral clusters, whereas that in the range of $\sim 470\text{ cm}^{-1}$ is attributed to the stretching mode of the octahedral clusters [18, 19]. The vibrational mode of the tetrahedral cluster is higher than that of octahedral mode due to shorter edge length of the tetrahedral clusters.

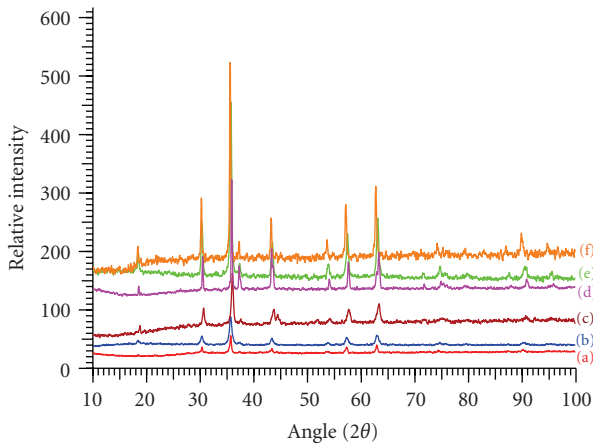
3.2. TEM Characterization. The TEM micrographs of all the samples exhibit highly agglomerated particles because of the interfacial surface tension as reported in our earlier studies [20–22]. As the annealing temperature increases from 400°C to 1000°C , the particle size increases from $\sim 10\text{ nm}$ to $\sim 45\text{ nm}$. Such an increase in grain size has also been reported earlier [23, 24]. It is widely believed that the net decrease in the solid-solid and solid-vapour interface free energy provides the driving force for grain growth during annealing process.

3.3. X-Ray Diffraction Studies. The typical X-ray diffraction patterns of the as-obtained $\text{CrCo}_{0.6}\text{Ni}_{0.4}\text{FeO}_4$ and those annealed at 400°C , 600°C , 800°C , and 1000°C for 2 hours are shown in Figure 1. The absence of any peak in the X-ray diffractograph of the as-obtained sample indicates the amorphous nature of the samples. However, the annealed samples exhibit characteristic diffraction peaks of the ferrite. The broad peaks at 400°C signify lower crystallite size of the synthesized sample and as the annealing temperature is increased, the peaks become sharp due to increase in the grain size.

The average crystallite size for all the samples has been calculated from the line broadening of the most intense peak corresponding to (3 1 1) plane of the spinel structure using the classical Scherrer equation [25]. It is observed that the particle size increases as the annealing temperature is raised

TABLE 1: Lattice parameters, saturation magnetization, coercivity, and energy band gap of the ferrites after annealing at 1000°C.

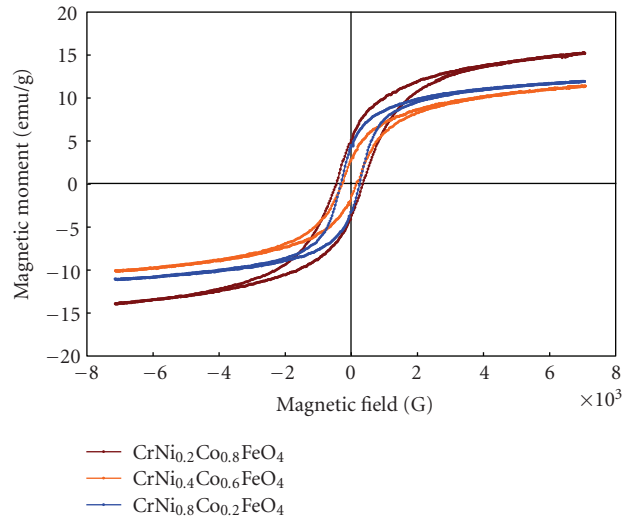
Ferrites composition	Lattice parameter, a (Å)	Volume (Å ³)	Saturation magnetization, M_s (emu/g)	Coercivity H_c (Oe)	Energy band gap, E_g (eV)
CrNiFeO ₄	8.2974	571.24	4.32	1500	2.30
CrNi _{0.8} Co _{0.2} FeO ₄	8.3026	572.32	9.75	290	2.27
CrNi _{0.6} Co _{0.4} FeO ₄	8.3143	574.75	14.86	240	2.73
CrNi _{0.4} Co _{0.6} FeO ₄	8.3321	578.45	17.70	190	2.82
CrNi _{0.2} Co _{0.8} FeO ₄	8.3567	583.59	19.85	130	2.62
CrCoFeO ₄	8.3736	587.13	13.28	38	2.50

FIGURE 2: X-ray diffraction patterns of (a) CrNi_{0.2}Co_{0.8}FeO₄, (b) CrNi_{0.4}Co_{0.6}FeO₄, (c) CrNi_{0.6}Co_{0.4}FeO₄, (d) CrNi_{0.8}Co_{0.2}FeO₄, (e) CrNiFeO₄, and (f) CrCrFeO₄ annealed at 1000°C.

from 400°C to 1000°C, which is also confirmed by the TEM studies.

Typical X-ray diffraction patterns for all the ferrites annealed at 1000°C for 2 hours are shown in Figure 2. All the samples have been found to be face centred cubic (fcc) with Fd-3m space group. The lattice parameters, calculated using Powley as well as Le-Bail refinement methods (built in TOPAS V2.1 of BRUKER AXS), are listed in Table 1. The lattice parameter “ a ” has been found to increase with cobalt concentration; this may be due to smaller ionic radius of nickel.

3.4. Magnetic Measurements. Hysteresis loops for all the samples annealed at 600°C and 1000°C are shown in Figures 3 and 4, respectively. It is observed that the saturation magnetization (M_s) increases with the annealing temperature due to increase in particle size [26]. From Table 1, it can be seen that the saturation magnetization, M_s , increases from 4.32 emu/g to 19.85 emu/g on increasing the cobalt concentration from 0 to 0.8. This increase can be understood because of the less magnetic behavior of nickel. However,

FIGURE 3: B-H loops of some typical CrCo _{x} Ni_{1- x} FeO₄ ferrites annealed at 600°C.

the saturation magnetisation decreases to 13.28 emu/g, with further increase of cobalt concentration to $x = 1.0$.

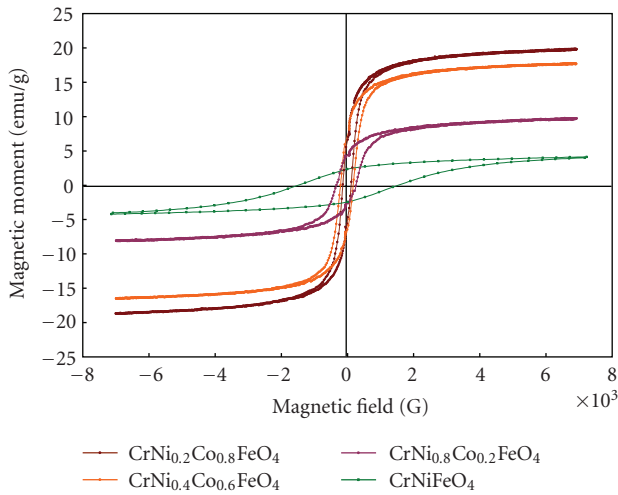
This behaviour can be explained on the basis of the super exchange interaction mechanism. In a cubic system of ferromagnetic spinels, the magnetic order is mainly due to super exchange interactions occurring between the metal ions in the A and B sublattices. Therefore, it is possible to vary magnetic properties of the samples by varying the cations. According to Neel’s two sublattice model of ferrimagnetism, the magnetic moment per formula unit (in μ_B), $n_B^N(x)$ is expressed as [27]

$$n_B^N(x) = M_B(x) - M_A(x), \quad (1)$$

where M_B and M_A are the B - and A -sublattice magnetic moments in μ_B , respectively. Cation distribution of the ferrites has been estimated using this model and is listed in Table 1, which suggests that cobalt and chromium ions predominantly occupy the octahedral sites, which is consistent with their preference for large octahedral site energy. This causes an increase in the saturation magnetization of the substituted ferrites up to $x = 0.8$. However, in the case

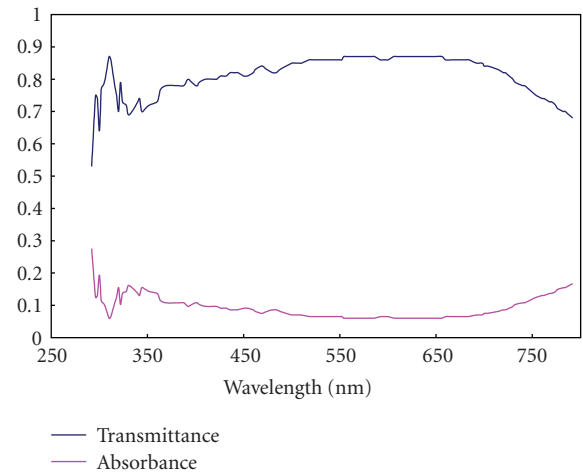
TABLE 2: Cation distribution for $\text{CrCo}_x\text{Ni}_{1-x}\text{FeO}_4$ annealed at 1000°C .

Ferrites Composition	Observed magnetic moment, (n_B)	Cation distribution	Calculated magnetic moment
CrNiFeO_4	0.18	$(\text{Fe}_{0.8}\text{Cr}_{0.2})^A[\text{NiCr}_{0.8}\text{Fe}_{0.2}]^B\text{O}_4$	0.20
$\text{CrNi}_{0.8}\text{Co}_{0.2}\text{FeO}_4$	0.40	$(\text{Fe}_{0.95}\text{Co}_{0.05})^A[\text{CrNi}_{0.8}\text{Co}_{0.15}\text{Fe}_{0.05}]^B\text{O}_4$	0.40
$\text{CrNi}_{0.6}\text{Co}_{0.4}\text{FeO}_4$	0.62	$(\text{Fe}_{0.95}\text{Co}_{0.05})^A[\text{CrNi}_{0.6}\text{Co}_{0.35}\text{Fe}_{0.05}]^B\text{O}_4$	0.60
$\text{CrNi}_{0.4}\text{Co}_{0.6}\text{FeO}_4$	0.73	$(\text{Fe}_{0.97}\text{Co}_{0.03})^A[\text{CrNi}_{0.4}\text{Co}_{0.57}\text{Fe}_{0.03}]^B\text{O}_4$	0.72
$\text{CrNi}_{0.2}\text{Co}_{0.8}\text{FeO}_4$	0.82	$(\text{Fe}_{0.99}\text{Co}_{0.01})^A[\text{CrNi}_{0.2}\text{Co}_{0.79}\text{Fe}_{0.01}]^B\text{O}_4$	0.84
CrCoFeO_4	0.58	$(\text{Fe})^A[\text{CoCr}]^B\text{O}_4$	1.00

FIGURE 4: B-H loops of some typical $\text{CrCo}_x\text{Ni}_{1-x}\text{FeO}_4$ ferrites annealed at 1000°C .

of CoCrFeO_4 saturation magnetization decreases because all the iron enters in to the A site. This may be due to the fact that the exchange interaction between A and B sites gets lowered resulting in strengthening of B - B interaction and weakening of A - B interaction, which leads to decrease of saturation magnetization. Therefore in CoCrFeO_4 Neel's magnetic moments calculated from expected cation distribution in comparison with that from the hysteresis loop do not give the satisfactory result.

The variation of the coercivity with average grain size has also been studied. It is observed that as the grain size increases, the value of coercivity (H_c), reaches a maximum value and then decreases. This variation of H_c with grain size can be explained on the basis of domain structure, critical diameter, and the anisotropy of the crystal [28, 29]. From Table 1, it is clear that the coercivity decreases with the decrease of nickel concentration. This may be attributed to the decrease in anisotropy field, which in turn decreases the domain wall energy [30, 31]. In the case of CrNiFeO_4 ,

FIGURE 5: Plot of absorbance and transmittance as a function of wavelength λ (nm) for $\text{CrCo}_{0.6}\text{Ni}_{0.4}\text{FeO}_4$ annealed at 1000°C .

the coercivity value is very high 1500 G. This behaviour in coercivity may be understood as described by the Banerjee and O'Reilly [32] on the basis of a new model for cation distribution. This may be due to the fact that the chromium ions enter into the tetrahedral site when $x > 0.8$. According to the cation distribution model [32] when Cr^{3+} ions occupy tetrahedral sites, they cause a negative trigonal field to be superimposed on the octahedral Cr^{3+} ions. Due to this a twofold degeneracy of the orbital ground state results in an unquenched orbital angular momentum and a large anisotropy.

3.5. Optical Studies. The energy band gaps of all the ferrites have been calculated with the help of optical absorption and percentage transmission data. The absorption and transmission spectra of $\text{CrCo}_{0.6}\text{Ni}_{0.4}\text{FeO}_4$ annealed at 1000°C are shown in Figure 5. The absorption coefficient, α of the nanoparticles has been calculated using the fundamental

relationships [33]

$$I = I_0 e^{-\alpha t},$$

$$A = \log \left(\frac{I_0}{I} \right), \quad \alpha = 2.303 (A/t), \quad (2)$$

where A is the absorbance and t is the thickness of the sample. To estimate the energy band gap for all the samples, the graph of $(\alpha h\nu)^2$ versus $h\nu$ has been plotted. The intercept of the line at $\alpha = 0$ gives the value of energy band gap. The values of energy band gap for all the samples annealed at 1000°C has been found to be in the range of 2.3–2.8 eV listed in Table 1. It is observed that as the particle size decreases, the energy band gap increases. This may be explained on the basis of Bras' effective mass model [34, 35] according to which the measured band gap, E_g can be expressed as a function of particle size as

$$E_g^* \cong E_g^{\text{bulk}} + \frac{\hbar^2 \pi^2}{2er^2} \left(\frac{1}{m_e} + \frac{1}{m_h} \right) - \frac{1.8e^2}{4\pi\epsilon\epsilon_0 r}, \quad (3)$$

where E_g^{bulk} is the bulk energy gap, r is the particle size, m_e is the effective mass of electrons, m_h is the effective mass of holes, ϵ is the relative permittivity, ϵ_0 is the permittivity of free space, \hbar is the planck's constant divided by 2π , and e is the charge on electron.

4. Conclusion

$\text{CrCo}_x\text{Ni}_{1-x}\text{FeO}_4$, $x = 0, 0.2, 0.4, 0.6, 0.8$ & 1.0 have been synthesized using the sol-gel autocombustion method. The formation of the ferrite powders has been confirmed by FT-IR and XRD studies. The TEM studies confirm that as the annealing temperature increases particle size increases up to 45 nm. The values of saturation magnetization increases and coercivity decreases with increasing Co^{3+} content. The values of energy band gap have been found to range ~2.5 eV. However, the band gap increases up to ~3.0 eV with the decrease of the particle size from ~45 nm to ~10 nm.

References

- [1] Y. Qi, Y. Yang, X. Zhao et al., "Controllable magnetic properties of cobalt ferrite particles derived from layered double hydroxide precursors," *Particuology*, vol. 8, pp. 207–211, 2010.
- [2] Y. Cedeño-Mattei and O. Perales-Pérez, "Synthesis of high-coercivity cobalt ferrite nanocrystals," *Microelectronics Journal*, vol. 40, no. 4-5, pp. 673–676, 2009.
- [3] J. Smit and H. P. J. Wijn, *Ferrites*, Philips Technical Library, Eindhoven, The Netherlands, 1959.
- [4] K. Ishino and Y. Narumiya, "Development of magnetic ferrites: control and application of losses," *American Ceramic Society Bulletin*, vol. 66, no. 10, pp. 1469–1474, 1987.
- [5] P. I. Slick, in *Ferromagnetic Materials*, E. P. Wohlfarth, Ed., vol. 2, p. 196, North-Holland, Amsterdam, The Netherlands, 1980.
- [6] T. Abraham, "Economics of ceramic magnets," *American Ceramic Society Bulletin*, vol. 73, no. 8, pp. 62–65, 1994.
- [7] D. Fiorani, in *Magnetic Properties of Fine Particles*, J. L. Dormann and D. Fiorani, Eds., North-Holland Delta Series, Elsevier, London, UK, 1992.
- [8] D. K. Kim, Y. Zhang, W. Voit, K. V. Rao, and M. Muhammed, "Synthesis and characterization of surfactant-coated superparamagnetic monodispersed iron oxide nanoparticles," *Journal of Magnetism and Magnetic Materials*, vol. 225, no. 1-2, pp. 30–36, 2001.
- [9] J. Smit and H. P. J. Wijn, *Ferrites*, John Wiley & Sons, London, UK, 1959.
- [10] S. H. Lee, S. J. Yoon, G. J. Lee et al., "Electrical and magnetic properties of $\text{NiCr}_x\text{Fe}_{2-x}\text{O}_4$ spinel ($0 \leq x \leq 0.6$)," *Materials Chemistry and Physics*, vol. 61, p. 147, 1999.
- [11] M. K. Fayek and S. S. Ata-Allah, "Fe Mössbauer and electrical studies of the (NiO)-(CrO)-(FeO) system," *Physica Status Solidi (A)*, vol. 198, no. 2, pp. 457–464, 2003.
- [12] A. M. Gismelseed and A. A. Yousif, "Mössbauer study of chromium-substituted nickel ferrites," *Physica B: Condensed Matter*, vol. 370, no. 1–4, pp. 215–222, 2005.
- [13] K. P. Chae, Y. B. Lee, J. G. Lee, and S. H. Lee, "Crystallographic and magnetic properties of $\text{CoCr}_x\text{Fe}_{2-x}\text{O}_4$ ferrite powders," *Journal of Magnetism and Magnetic Materials*, vol. 220, no. 1, pp. 59–64, 2000.
- [14] M. A. Gabal and Y. M. A. Angari, "Effect of chromium ion substitution on the electromagnetic properties of nickel ferrite," *Materials Chemistry and Physics*, vol. 118, no. 1, pp. 153–160, 2009.
- [15] N. A. Chen, K. Yang, and M. Gu, "Microwave absorption properties of La-substituted M-type strontium ferrites," *Journal of Alloys and Compounds*, vol. 490, no. 1-2, pp. 609–612, 2010.
- [16] S. E. Jacobo, C. Herme, and P. G. Bercoff, "Influence of the iron content on the formation process of substituted Co-Nd strontium hexaferrite prepared by the citrate precursor method," *Journal of Alloys and Compounds*, vol. 495, no. 2, pp. 513–515, 2010.
- [17] Q. Fang, H. Cheng, K. Huang, J. Wang, R. Li, and Y. Jiao, "Doping effect on crystal structure and magnetic properties of chromium-substituted strontium hexaferrite nanoparticles," *Journal of Magnetism and Magnetic Materials*, vol. 294, no. 3, pp. 281–286, 2005.
- [18] A. Pradeep and G. Chandrasekaran, "FTIR study of Ni, Cu and Zn substituted nano-particles of MgFe_2O_4 ," *Materials Letters*, vol. 60, no. 3, pp. 371–374, 2006.
- [19] P. N. Vasambekar, C. B. Kolekar, and A. S. Vaingankar, "Magnetic behaviour of Cd and Cr substituted cobalt ferrites," *Materials Chemistry and Physics*, vol. 60, no. 3, pp. 282–285, 1999.
- [20] S. Singhal, A. N. Garg, and K. Chandra, "Evolution of the magnetic properties during the thermal treatment of nanosize BaMFeO ($M = \text{Fe, Co, Ni}$ and Al) obtained through aerosol route," *Journal of Magnetism and Magnetic Materials*, vol. 285, no. 1-2, pp. 193–198, 2005.
- [21] S. Singhal, J. Singh, S. K. Barthwal, and K. Chandra, "Preparation and characterization of nanosize nickel-substituted cobalt ferrites (CoNiFeO)," *Journal of Solid State Chemistry*, vol. 178, no. 10, pp. 3183–3189, 2005.
- [22] S. Singhal and K. Chandra, "Cation distribution and magnetic properties in chromium-substituted nickel ferrites prepared using aerosol route," *Journal of Solid State Chemistry*, vol. 180, no. 1, pp. 296–300, 2007.
- [23] A. C. F. M. Costa, A. P. Diniz, V. J. Silva et al., "Influence of calcination temperature on the morphology and magnetic properties of Ni-Zn ferrite applied as an electromagnetic energy absorber," *Journal of Alloys and Compounds*, vol. 483, no. 1-2, pp. 563–565, 2009.
- [24] J. E. Burke and D. Turnbull, "Recrystallization and grain growth," *Progress in Metal Physics*, vol. 3, p. 220, 1952.

- [25] B. D. Cullity, *Elements of X-Ray Diffraction*, chapter 14, Addison-Wesley, Reading, Mass, USA, 1976.
- [26] B. S. Chauhan, R. Kumar, K. M. Jadhav, and M. Singh, "Magnetic study of substituted mg-mn ferrites synthesized by citrate precursor method," *Journal of Magnetism and Magnetic Materials*, vol. 283, no. 1, pp. 71–81, 2004.
- [27] L. Neel, *Comptes Rendus de l'Académie des Sciences*, vol. 230, p. 375, 1950.
- [28] S. Singhal, T. Namgyal, S. Bansal, and K Chandra, "Effect of Zn Substitution on the Magnetic Properties of Cobalt Ferrite Nano Particles Prepared Via Sol-Gel Route," *Journal of Electromagnetic Analysis and Application*, vol. 2, p. 376, 2010.
- [29] B. D. Cullity, *Introduction to Magnetic Materials*, Addison-Wesley, Reading, Mass, USA, 1972.
- [30] Y. M. Yakovlev, E. V. Rubalikaya, and N. Lapovok, "Ferromagnetic Resonance in Lithium Ferrite," *Soviet Physics-Solid State*, vol. 10, p. 2301, 1969.
- [31] K. S. Rao, A. M. Kumar, M. C. Varma, G. S. V. R. K. Choudary, and K. H. Rao, "Cation distribution of titanium substituted cobalt ferrites," *Journal of Alloys and Compounds*, vol. 488, no. 1, pp. L6–L9, 2009.
- [32] S. K. Banerjee and W. O'Reilly, *IEEE Transactions on Magnetics*, vol. 3, p. 463, 1966.
- [33] M. Srivastava, A. K. Ojha, S. Chaubey, and A. Materny, "Synthesis and optical characterization of nanocrystalline NiFeO structures," *Journal of Alloys and Compounds*, vol. 481, no. 1-2, pp. 515–519, 2009.
- [34] K. F. Lin, H. M. Cheng, H. C. Hsu, LI. J. Lin, and W. F. Hsieh, "Band gap variation of size-controlled ZnO quantum dots synthesized by sol-gel method," *Chemical Physics Letters*, vol. 409, no. 4-6, pp. 208–211, 2005.
- [35] O. S. Polezhaeva, N. V. Yaroshinskaya, and V. K. Ivanov, "Synthesis of nanosized ceria with controlled particle sizes and bandgap widths," *Russian Journal of Inorganic Chemistry*, vol. 52, no. 8, pp. 1184–1188, 2007.



Hindawi

Submit your manuscripts at
<http://www.hindawi.com>

